Trends in Genetics

CellPress

Review

Update: Mechanisms Underlying N^6-Methyladenosine Modification of Eukaryotic mRNA

Yang Wang[1] and Jing Crystal Zhao[1,*]

Eukaryotic mRNA undergoes chemical modification both at the 5′ cap and internally. Among internal modifications, N^6-methyladensone (m^6A), by far the most abundant, is present in all eukaryotes examined so far, including mammals, flies, plants, and yeast. m^6A modification has an essential role in diverse biological processes. Over the past few years, our knowledge relevant to the establishment and function of this modification has grown rapidly. In this review, we focus on technologies that have facilitated m^6A detection in mRNAs, the identification of m^6A methylation enzymes and binding proteins, and potential functions of the modification at the molecular level.

Methods to Detect m^6A

Historically, methods used to detect and quantify overall m^6A levels on mRNA have included chromatography [1–4], 2D cellulose thin-layer chromatography (2D-TLC) [5,6], dot-blotting [7], and liquid chromatography-tandem mass spectrometry (LC-MS/MS) [7] (Table 1). Based on these studies, it is now accepted that the m^6A frequency is three to five residues per mRNA [1–3,8–10]. However, methods used until recently could not reveal m^6A location, a task that has proven challenging. Although the m^6A methyl group is found at the Watson–Crick base-pairing site and perturbs adenosine and uridine (A/U) or A/T (thymidine) pairing, it does not completely block reverse transcriptase, as m^1A RNA modification does [11], and there is no chemical treatment analogous to bisulfite conversion of 5mC available to convert m^6A to a different and detectable nucleotide [12]. Therefore, it remained unclear for a long time which mRNAs even exhibit m^6A.

However, in 2012, two groups independently developed technology that coupled RNA immunoprecipitation using an m^6A-specific antibody to next-generation high-throughput sequencing (m^6A meRIP-Seq) to map m^6A sites in the mammalian transcriptome [13,14] (Table 1). Initially, m^6A was mapped to over 7000 coding and noncoding mammalian polyadenylated (polyA) RNAs [13,14]. Since then, over 10 000 m^6A-methylated polyA RNAs have been reported from various organisms and cell types, from yeast to mammalian reprogrammed pluripotent stem cells [13–23]. A consensus m^6A methylation motif, RRACH (R = G or A; H = A, C or U), was identified from high-throughput data [13,14], in agreement with biochemical studies [24–26]. Recently, the consensus motif was redefined as DRACH (D = A, G or U), based on a study reporting that the nucleotide at the –2 position relative to m^6A can also be U [22]. Many m^6A sites are highly conserved between species, suggesting the evolutionary importance of the

Trends

m^6A is the most abundant internal mRNA modification that tags tens of thousands eukaryotic transcripts. Technologies to detect m^6A have improved rapidly. Now we can map m^6A methylome at a single nucleotide resolution and determine the proportion of methylated versus unmethylated transcripts in a high-throughput manner.

The 'writer', 'eraser', and 'reader' of m^6A modification have been reported. These discoveries have greatly facilitated our understanding of the functional significance of m^6A.

Emerging evidence suggests that m^6A has critical roles in regulating diverse mRNA activities, from processing to localization and translation. Therefore, reversible m^6A modification represents a new and crucial layer of gene expression regulation in eukaryotes.

[1]Tumor Initiation And Maintenance Program, Sanford Burnham Prebys Medical Discovery Institute, La Jolla, CA 92037, USA

*Correspondence: czhao@sbpdiscovery.org (J.C. Zhao).

Table 1. Methods Used to Detect and Map m^6A Modification of Polyadenylated RNA

Method	Purpose	Pros	Cons	Refs
2D-TLC	Measure overall m^6A levels	Well-established protocol; quantitative; high sensitivity	Requires radioactivity; does not cover all A sites due to specificity of ribonucleases used for 5′ end labeling	[5,6]
LC-MS/MS		Quantitative; covers all A sites; very high sensitivity	Requires special equipment and expertise; high cost	[7]
Dot blot		Low cost; no radioactivity required	Nonspecific antibody binding; low sensitivity	[7]
Ligation assay	Measure m^6A levels at a specific site	Easy to set up	Not applicable to endogenous m^6A sites; requires radioactivity	[39]
Primer extension		Easy to set up	Relies on specific reverse transcriptase; cannot detect low-abundance m^6A sites	[37]
SMRT		Single-molecule, real-time detection	Requires special equipment; quantification not reported	[38]
SCARLET		Precise locations mapped; highly quantitative	Requires radioactivity and sophisticated methodology	[40]
m^6A-meRIP-Seq	Map m^6A locations genome wide	Well-established protocol; high sensitivity	Immunoprecipitation/antibody can yield false positives; low resolution	[13,14]
PA-m^6A-RIP-Seq		Higher resolution than meRIP-seq	Need to use living cells to incorporate 4-SU; thus cannot be applied to tissue or clinical samples; immunoprecipitation/antibody can yield false positives	[20]
miCLIP-Seq		Single-nucleotide resolution	High reliance on specific antibody to generate a signature at m^6A sites	[21,22]
m^6A-LAIC-seq		Only method to quantify percentage of methylated versus unmethylated RNAs	Cannot detect specific m^6A sites	[23]
Two-color microarray		Antibody not required	Low sensitivity	[31]

modification [13,14]. There is general agreement that m^6A is highly enriched at 3′ untranslated regions (UTRs) [13,14,20–22], and early meRIP-seq studies suggested that m^6A is located near stop codons [13,14,16]. However, a later study with improved detection resolution suggested that m^6A sites are present in 3′-UTR, but there is no preference for m^6A to locate around stop codons [21]. Some m^6A modifications have also been found flanking 5′- and 3′-splice sites of exons, spatially overlapping with binding sites for mRNA splicing factors [27,28], suggestive of a splicing function. Since N^6, 2′-O-dimethyladenosine (m^6Am), a modification that occurs exclusively on the first nucleotide of mRNAs [29], can also be recognized by anti-m^6A antibody, m^6A abundance at 5′-UTRs remained unclear until a recent study distinguished these modifications using improved technology. This study showed m^6Am enrichment at transcription start sites [22]. By contrast, lower m^6A levels were detected at 5′-UTRs [22]. Nevertheless, the same group later reported that m^6A but not m^6Am at the 5′-UTR regulates cap-independent mRNA translation [30].

One limitation of the original meRIP-seq method is its relatively low resolution: m^6A can be mapped within a 100–200-nucleotide transcript region but precise positions cannot be identified

[13,14]. Efforts from multiple laboratories have improved meRIP-seq resolution. Using yeast as a system, one study employed an improved computational algorithm to predict m^6A at almost single-nucleotide resolution [15]. Additionally, a photo-crosslinking-assisted m^6A sequencing strategy (PA-m^6A -seq) has been used to improve resolution [20] (Table 1). In 2015, two groups adapted ultraviolet (UV) CLIP (crosslinking immunoprecipitation) to accurately locate tens of thousands of m^6A residues in mammalian mRNAs with single-nucleotide resolution [21,22] (Table 1). Both studies screened different m^6A antibodies and found that some can induce specific mutational signatures around m^6A residues after UV light-induced antibody/RNA cross-linking and reverse transcription. This approach can map m^6A at single-nucleotide resolution.

Another limitation of meRIP-seq m^6A detection methods is their reliance on antibody-based IP procedures, which are often associated with false positives [15]. To circumvent this problem, alternative technologies have been developed. These include m^6A detection by: (i) two-color tiling microarray [31] based on m^6A interference with A/T pairing [32–36] (Table 1); (ii) reverse transcription-based methods, based on changes in kinetics of specific reverse transcriptases by m^6A base modifications [37,38] (Table 1); and (iii) ligation-based assays, such as site-specific cleavage and radioactive-labeling followed by ligation-assisted extraction and thin-layer chromatography (SCARLET) [39,40] (Table 1). Although these methods cannot yet be carried out in a high-throughput manner comparable with meRIP-seq and some are applicable to only specific transcripts, they provide a complementary approach to confirm specific m^6A sites identified by meRIP-seq.

An important question is, among the sites modified by m^6A, what fraction of transcripts are m^6A tagged versus untagged? For example, for the long noncoding RNA (lncRNA) metastasis-associated lung adenocarcinoma transcript 1 (*MALAT1*) four precise m^6A sites were mapped using SCARLET technology [40]. The proportion of *MALAT1* transcripts modified at these sites varies between 11% and 77% in HeLa cells, suggesting that variation in modification of a potential m^6A site could have functional consequences for methylated versus unmethylated RNAs. Recently, one group developed a technology termed 'm^6A-level and isoform-characterization-sequencing' (m^6A-LAIC-seq) to detect m^6A methylated versus unmethylated mRNA transcripts [23] (Table 1). The m^6A-LAIC-seq method modifies the standard m^6A-meRIP-seq protocol by using excess m^6A antibody, including RNA spike-in controls to improve quantification, and sequencing full-length rather than fragmented PolyA RNAs. Use of excess m^6A antibody and full-length transcripts ensures that all m^6A -containing PolyA RNAs are pulled down in the immunoprecipitated fraction and not in the flow-through. Therefore, the proportion of PolyA RNAs containing m^6A is calculated as the ratio of transcripts detected in the immunoprecipitated versus flow-through fractions. The authors reported that, for most genes, less than 50% of transcripts contained m^6A methylation and proportions differed between cell types. This method quantified for the first time the proportion of m^6A methylated versus unmethylated transcripts on a genome-wide scale. However, since full-length mRNAs were used, m^6A locations were not defined; thus the resolution of this method is at the mRNA rather than the m^6A site level. Furthermore, this method cannot distinguish m^6Am- from m^6A-containing mRNAs. Hence, novel methods are required to map fraction of specific m^6A sites.

m^6A Methyltransferases and Demethylases

m^6A is a reversible modification. An effort to purify enzymes that synthesize m^6A began during the 1990s [41,42]. Methyltransferase-like 3 or METTL3 (also known as MTA-70) was reported as a putative m^6A methyltransferase in 1997 [43]. Not until 2014 did four studies [17,19,28,44] report significant interaction between METTL3 and the previously uncharacterized protein METTL14, which also harbors an MTA domain [17,19,28,44,45]. Two of the studies reported that a combination of METTL3 and METTL14 showed remarkably greater *in vitro* methyltransferase activity than did METTL3 or METTL14 alone, suggesting that they functioned synergistically [19,44] (Figure 1). This prediction was confirmed by recent reports of the crystal structure of

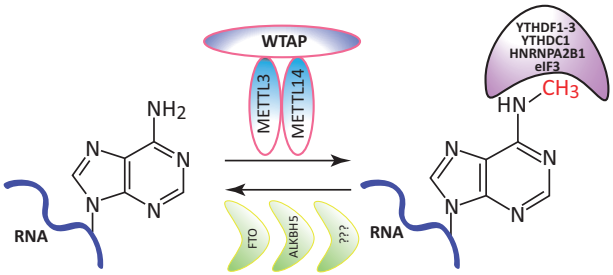

Figure 1. Formation, Removal, and Recognition of N^6-Methyladensone (m^6A). Methyltransferase-like 3 (METTL3)/METTL14 were identified as core components of an m^6A methyltransferase complex. Both form a heterodimer catalyzing m^6A formation. Wilms tumor 1-associated protein (WTAP) has been identified as a METTL3- and METTL14-interacting protein. The presence of WTAP does not alter METTL3/METTL14 methyltransferase activity *in vitro*, but WTAP has a critical role in m^6A formation *in vivo* through an as yet unknown mechanism. Other METTL3/METTL14-interacting proteins have been identified, but their activities remain to be determined. Two AlkB family members, Fat mass and obesity-associated protein (FTO) and Alkylation Repair Homolog 5 (ALKBH5), reportedly serve as m^6A demethylases and remove m^6A in an oxidative manner, although additional unknown m^6A demethylases may also serve this function. Several m^6A-binding proteins are reported, including multiple YTH family members (YTHDF1-3 and YTHDC1), heterogeneous ribonucleoprotein HNRNPA2B1, and eukaryotic initiation factor 3 (eIF3).

a METTL3/METTL14 heterodimer [46–48]. Those studies focused on the METTL3 or METTL14 methyltransferase domain and adjacent motifs and were based on ligand-free, methyl group donor *S*-adenosyl methionine (SAM)-bound states [46–48]. Interestingly, previous studies [19,44] reported that METTL14 displayed higher methyltransferase activity than did METTL3 in *in vitro* methylation assays, suggesting METTL14 as the predominant catalytic subunit. By contrast, structural analysis supports a model in which METTL3 serves as the catalytic subunit, which binds SAM, while METTL14 has a structural role and potentially functions in RNA substrate binding via the positively charged groove formed between METTL3 and METTL14 [46–48]. One particular structural study suggested that, while both METTL3 and METTL14 display a predicted catalytic motif, the METTL14 SAM-binding domain is blocked, while that of METTL3 is hollow, allowing binding [47]. The authors of that study suggested that high METTL14 activity in a methylation assay was due to METTL3 contamination [47], explaining conflicting conclusions emerging from biochemical versus structural studies. As yet, the structure of a METTL3/METTL14 RNA complex has not been solved, an achievement that would provide important information relevant to substrate sequence specificity.

The RRACH motif has been identified as being enriched at m^6A sites; however, only a small fraction of RRACH motifs exhibit m^6A [13,14]. How METTL3/METTL14 is recruited to a specific transcript and why some RRACH motifs become modified and others do not remains poorly understood. It is hypothesized that RNA-binding proteins (RBPs) interacting with METTL3/METTL14 may recruit these proteins. Several METTL3/METTL14-interacting proteins have been identified. The most well established is Wilms tumor 1-associated protein (WTAP), which is an RBP that displays high affinity to METTL3/METTL14 [17,28] (Figure 1). METTL3/WTAP interactions are conserved in yeast [49]. Although WTAP does not alter METTL3/METTL14 methyltransferase activity *in vitro*, its loss promotes transcriptome-wide m^6A depletion in cells [17,28], demonstrating that it is required for m^6A modification and suggesting that it directs METTL3/METTL14 onto targets via RNA-binding activity. Indeed, WTAP PAR-CLIP analysis reported direct WTAP binding to RNA and m^6A enrichment at WTAP/RNA-binding sites [28]. Nonetheless, how WTAP recognizes RRACH motifs and facilitates methylation of adenosine within them is unknown. In addition to WTAP, 13 other proteins have been identified in a METTL3-interacting protein network [17]. Knockdown of one, *KIAA1429*, decreased the global m^6A levels [17]. Functions of other proteins identified in the network remain unknown.

m^{6}A methyl groups are removed by m^{6}A demethylase (Figure 1). Two members of the alpha-ketoglutarate-dependent dioxygenase AlkB family, Fat mass and obesity-associated protein (FTO) and Alkylation Repair Homolog 5 (ALKBH5), reportedly remove m^{6}A in an oxidative manner [7,50]. FTO was first shown to demethylate 3-methylthymine on single-stranded DNA (ssDNA) [51]. Later, a group showed that FTO demethylates 3-methyluridine in ssRNA [52] *in vitro*. In 2011, the same group reported that m^{6}A -modified RNA was the primary FTO substrate [7]. Overexpression of FTO or ALKBH5 in cells decreases global m^{6}A levels, but knockdown or knockout of either only mildly increases m^{6}A levels [7,50], suggesting the existence of other demethylases or perhaps a synergy between ALKBH5 and FTO that has not yet been studied. The crystal structures of both FTO and ALKBH5 have been reported, and small-molecule inhibitors targeting their demethylase activities have been developed based on these structures [53–55]. For example, the natural product rhein, derived from herbs, is among the most effective FTO m^{6}A demethylase inhibitors [56]. As yet, it is unclear whether FTO or ALKBH5 target the same or different methylated mRNAs.

m^{6}A-Binding Proteins

Similar to methylated DNA and histone protein tails, m^{6}A-modified RNA is recognized by specific proteins, or readers, that transmit the code to downstream effectors. In 2012, using methylated versus non-methylated RNA probes as baits, several m^{6}A-interacting proteins in mammalian cells, including members of the YTH domain-containing family, such as YTHDF2 and YTHDF3, were pulled down [14] (Figure 1). Later, a study demonstrated direct binding of YTHDF2 to m^{6}A RNA [18]. Since then, additional YTH family proteins have been identified as m^{6}A binders, including YTHDF1 and YTHDC1 [57–59]. In agreement, while biochemical and structural analysis revealed YTH as a general RNA-binding domain [60], kinetic analysis demonstrated that the binding affinity between YTH domains to m^{6}A-modified RNA was ten times higher than that to non-m^{6}A RNA [61,62]. Furthermore, PAR-CLIP analysis of YTHDF1, YTHDF2, and YTHDC1 identified genome-wide YTH protein-binding sites overlapping with the RRACH motif [18,57,58]. Together, these studies strongly support the direct interaction of YTH proteins and m^{6}A-modified RNA. However, it is noteworthy that YTH domain affinity for m^{6}A is moderate and lower than that of DNA methylation-binding proteins, such as Methyl-CpG-binding domain protein 1 (MBD1) and Methyl-CpG-binding protein 2 (Mecp2) for 5mC [63]. In addition, YTHDF1/2 CLIP-seq data clearly showed that YTH proteins also bind to RNA sites that lack m^{6}A *in vivo* [18,58]. Therefore, observations derived from these studies, which have greatly advanced our knowledge of how m^{6}A exerts its function, underscore the importance of using cells engineered to lack m^{6}A as controls in analyzing YTH domain protein function in m^{6}A modification to ensure specificity of effects. While YTHDF1/2 proteins are generally defined as cytoplasmic m^{6}A 'readers', YTHDC1 is a nuclear reader. A different nuclear m^{6}A-binding protein was recently reported, the heterogeneous ribonucleoprotein HNRNPA2B1 [64] (Figure 1). m^{6}A also reportedly binds eukaryotic initiation factor 3 (eIF3), a critical component of translation initiation complex [30] (Figure 1). The proposed functions of these binding are discussed below.

m^{6}A Regulates mRNA Activity through Diverse Mechanisms

m^{6}A Destabilizes RNA

Early studies during the 1970s hinted that RNA methylation functions in regulating mRNA stability [10,65]. Multiple recent studies have reported that the loss of m^{6}A methyltransferase activity accompanied by decreased m^{6}A modification increases transcript stability [16–19,66], suggesting that m^{6}A modification destabilizes RNA (Figure 2, Key Figure). Multiple underlying mechanisms have been proposed.

One study reported that YTHDF2 binds to m^{6}A, which then translocates mRNA from the translation machinery to processing bodies (P-bodies), where it is degraded [18]. However, a later study challenged this model by showing that YTHDF2 does not interact with core

Key Figure

Diverse Molecular Mechanisms of N^6-Methyladensone (m^6A)

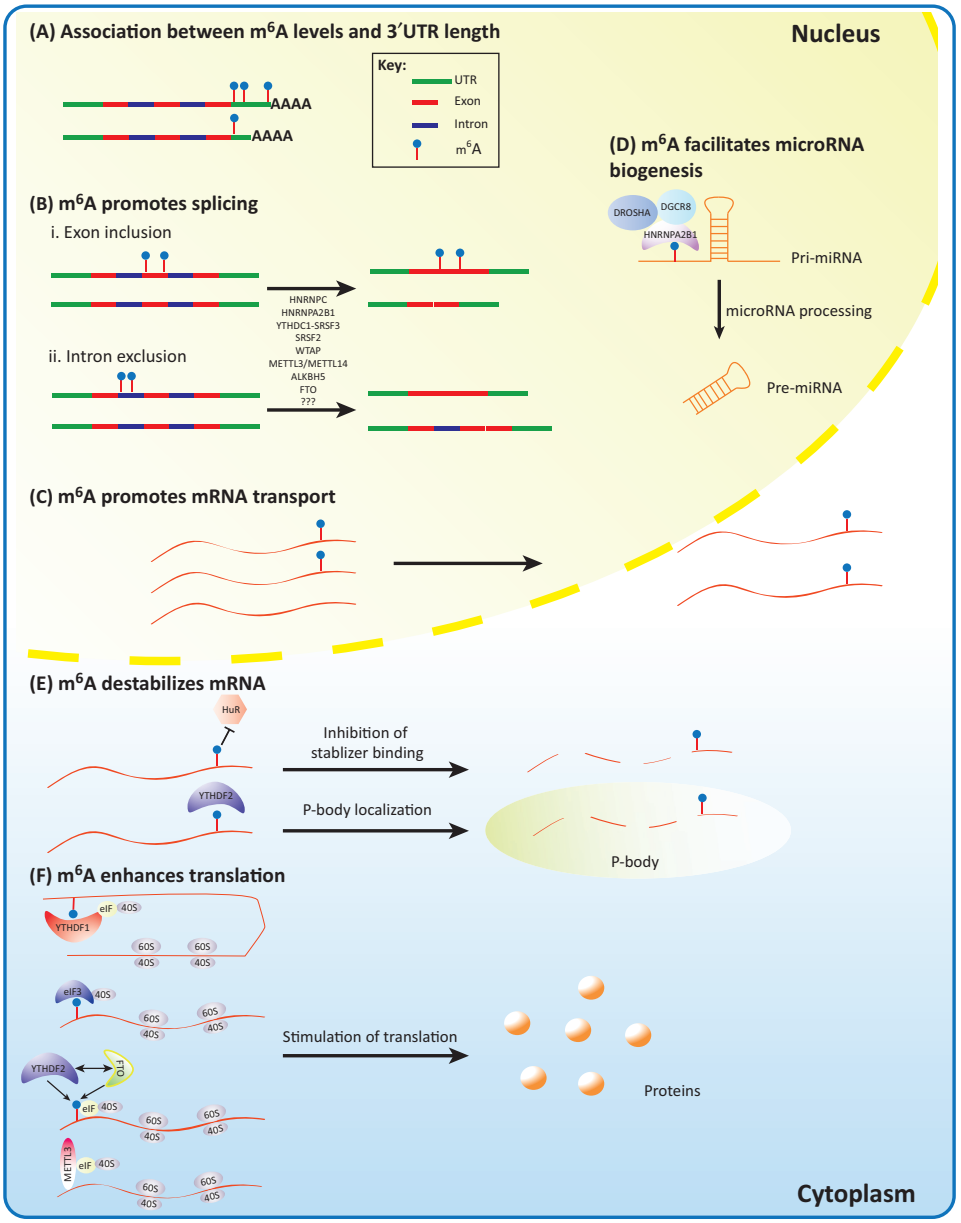

Figure 2. (A) Association between m^6A levels and 3′ untranslated region (UTR) length; (B) m^6A promotes splicing; (C) m^6A promotes mRNA transport; (D) m^6A facilitates miRNA biogenesis; (E) m^6A destabilizes mRNA; and (F) m^6A enhances translation. As indicated, these activities occur in the nucleus, cytoplasm, or both.

components of the P-body and that, instead, YTHDF2 directly recruits the CCR4-NOT deadenylase complex to destabilize RNAs that contain m^{6}A [67]. These discrepant findings may reflect direct and indirect mechanisms on YTHDF2 regulated m^{6}A-mRNA stability. In addition to YTHDF2, two groups reported that all three YTHDF proteins (YTHDF1-3) regulate HIV-1 RNA expression; one study reported that all three promoted HIV-1 RNA expression [68], while the other reported that they repress HIV-1 RNA expression [69]. One thing that both studies agree on is that all three YTHDF proteins regulate gene expression in the same manner, in contrast to previous studies reporting that YTHDF2 destabilizes mRNA [18], while YTHDF1 promotes protein synthesis [58]. These differences may reflect genome-wide versus gene-specific effects, but warrant future investigation.

Another study showed that m^{6}A blocks mRNA binding to the mRNA stabilizer human antigen R (HuR or ELAVL1) [19]. In that study, the authors observed that whether m^{6}A blocks or facilitates mRNA and HuR interaction depends on the distance between m^{6}A and HuR-binding sites [19]. When sites are in close proximity, m^{6}A promotes HuR binding, consistent with previous work that identified HuR as a m^{6}A-binding protein by using an m^{6}A site probe next to a HuR-binding U track [14]; by contrast, when m^{6}A and HuR binding sites were far apart, the presence of m^{6}A decreased HuR binding [19]. Since predicted RNA motifs favoring m^{6}A modification or HuR binding differ substantially in sequence, endogenous m^{6}A and HuR sites may not always colocalize. Thus, it was proposed that m^{6}A is more likely to block HuR-RNA binding, destabilizing mRNA *in vivo*. Since this work was not performed on a transcriptome-wide scale, future studies should address the scope of this interaction.

m^{6}A Alters RNA Structure to Modulate RNA/Protein Interactions

It is well established that secondary and tertiary structures govern RNA function [70,71]. Since m^{6}A destabilizes A/U pairing [31–36], it is reasonable to predict that m^{6}A can alter the thermostability of an RNA duplex to change RNA secondary structure and function. Indeed, using a technology known as *in vivo* click selective 2′-hydroxyl acylation and profiling experiment (icSHAPE), which can determine endogenous RNA secondary structure, one group compared RNA base-pairing status of the m^{6}A consensus motif GGACU in wildtype versus *METTL3*-knockout mouse embryonic stem cells (mESCs) [72]. They reported that the GGACU motif is less structured in wildtype ESCs than in ESCs lacking m^{6}A, suggesting that m^{6}A helps transit paired RNA to unpaired RNA [72]. Another study further demonstrated that m^{6}A-mediated RNA structural changes alter RNA/protein interactions [73]. These authors reported that m^{6}A on a stem-loop region of the lncRNA *MALAT1* altered local RNA structure to enhance *MALAT1* binding to the RBP heterogeneous nuclear ribonucleoprotein C (HNRNPC). They named this type of m^{6}A-containing region an 'm^{6}A-switch' and identified thousands of potential RNA sequences that could function in a 'switch' using sequential HNRNPC-PAR-CLIP followed by m^{6}A-RIP-Seq in wildtype versus *METTL3*/*METTL14*-knockdown cells. Most switches were located in introns of coding and ncRNAs and potentially regulate alternative splicing [73].

m^{6}A Enhances mRNA Translation

Several mechanisms have been proposed relevant to m^{6}A effects on translation (Figure 2). In 2015, a study reported that the m^{6}A-binding protein YTHDF1 interacts with eIF3 to promote efficient translation of m^{6}A -modified mRNAs [58]. Later, two studies reported that cellular stress, such as heat shock, increases m^{6}A modification at mRNA 5′-UTRs and promotes mRNA translation [30,74]. One study showed that m^{6}A promoted cap-independent mRNA translation in the absence of the cap-binding factor eIF4E, since m^{6}A directly binds eIF3 to recruit the 43S complex, initiating translation [30]. The other study showed that, in the nucleus, heat shock-induced 5′-m^{6}A was protected from FTO-mediated demethylation by nuclear-translocated YTHDF2 [74]. This model is supported by observations that the affinity of m^{6}A RNA for the YTH domain is greater than that of m^{6}A RNA for FTO [61,62,75]. Yet another study reported that

METTL3 directly interacts with the translation initiation factor eIF3 to promote translation of a subset of mRNAs, independent of METTL3 methyltransferase activity or YTHDF1 or YTHDF2 binding [76]. It remains unclear whether and how these mechanisms coexist in cells. It would now be informative to identify RNA substrates for each of these mechanisms to understand the significance of each in normal or conditioned, such as heat-shocked, cells.

About half of mammalian m^{6}A sites are located in coding sequence [13]. One study used biochemical, structural, and single-molecule methods to address the function of m^{6}A modification in mRNA/tRNA interactions using *Escherichia coli* ribosomes as a system [77]. The authors showed that, although X-ray crystallographic analyses indicate that m^{6}A base-pairs with uridine during the decoding process, m^{6}A modification can act as a barrier to tRNA accommodation and translation elongation in a manner that depends on the position and context of m^{6}A within codons [77]. These authors proposed that such dynamic changes could modulate coupled co-translational processes, such as protein folding, suggesting that m^{6}A allows a single gene to encode proteins of different functional forms.

m^{6}A Promotes Exon Inclusion and Enhances mRNA Splicing

m^{6}A-related proteins, including METTL3/METTL14/WTAP of the methyltransferase complex, FTO and ALKBH5 demethylases, or m^{6}A binding proteins YTHDF2 and YTHDC1, all reportedly localize in nuclear organelles known as speckles, which are enriched in pre-mRNA splicing factors [7,18,28,43,50,59], suggesting a role for m^{6}A RNA modification in mRNA splicing (Figure 2). Within the METTL3/METTL14/WTAP complex, WTAP is required for METTL3 and METTL14 accumulation in nuclear speckles and most mRNA species bound by WTAP and METTL14 were transcribed from genes known to give rise to mRNAs with multiple splicing variants [28]. Loss-of-function studies further showed that depletion of either METTL3 or WTAP results in transcriptome-wide changes in RNA splicing [28,64]. Together, these data suggest that m^{6}A methyltransferase activity regulates mRNA splicing.

One study reported that FTO depletion enhances m^{6}A levels in regions flanking 5′- and 3′-splice sites and promotes binding of the splicing factor SRSF2, increasing exon inclusion [78]. *ALKBH5*-knockdown cells show loss of phosphorylated SC35, a marker of nuclear speckles, suggesting that ALKBH5 regulates speckle formation, an effect dependent on ALKBH5 demethylase activity [50].

The m^{6}A nuclear reader YTHDC1 reportedly binds the pre-mRNA splicing factors SRSF3 and SRSF10 competitively, and promotes exon inclusion by facilitating SRSF3 but repressing SRSF10 in their nuclear speckle localization and RNA binding [59]. Another nuclear m^{6}A reader HNRNPA2B1 reportedly directly binds a set of m^{6}A-tagged nuclear transcripts and modulates their splicing in a manner comparable with METTL3, as evidenced by a strong positive correlation between global changes in alternative splicing and depletion of either HNRNPA2B1 or METTL3 [64].

m^{6}A Promotes mRNA Transport into the Cytoplasm

ALKBH5-knockout mice showed moderate increases in m^{6}A levels and accelerated mRNA export to the cytoplasm [50] (Figure 2). As a mechanism, the authors of that study focused on the splicing factor Alternative splicing factor (ASF/SF2), because it colocalizes with ALBKH5 in nuclear speckles [50]. It is also well established that ASF/SF2 hypophosphorylation switches its function from that of a splicing factor to an adaptor protein functioning in mRNA nuclear export [79,80]. Interestingly, ALKBH5-deficient cells not only show ASF/SF2 hypophosphorylation and loss of ASF localization to nuclear speckles, but also relocalization of the ASF/SF2 kinase Serine/threonine-protein kinase 1 (SRPK1) from the nucleus to the cytoplasm. Thus, the authors proposed that SRPK1 relocation underlies ASF/SF2 hypophosphorylation, enhancing mRNA

transport to the cytoplasm. Importantly, the observed phenotypes in *ALKBH5*-knockout cells can only be rescued by the overexpression of wildtype but not mutant ALKBH5 lacking demethylase activity, suggesting that m^{6}A modification regulates mRNA transport. However, the exact mechanism remains unclear.

m^{6}A Levels Are Associated with Usage of Alternative PolyA Sites

A UV CLIP study that mapped m^{6}A sites in the mammalian transcriptome at single-nucleotide resolution reported a positive correlation between m^{6}A density and the length of the last exon [21] (Figure 2). The authors then simultaneously knocked down *METTL3*, *METTL14*, and *WTAP* and examined alternative polyA (APA) usage in a subset of mRNAs. They found that, following the global reduction of m^{6}A levels, a greater number of genes showed proximal APA usage, raising the possibility that some m^{6}A residues inhibit proximal polyadenylation. In agreement, another study measured the fraction of m^{6}A-methylated versus nonmethylated RNAs and reported that m^{6}A levels were positively correlated with 3′-UTR length [23]. However, mechanisms underlying these activities remain undetermined.

An Interaction between m^{6}A Modification and the miRNA Pathway

It was reported that METTL3-mediated m^{6}A methylation of primary miRNAs facilitated primary miRNA processing by the DGCR8 microprocessor complex [81] (Figure 2). This group further identified HNRNPA2B1 as a nuclear m^{6}A reader mediating this process [64]. Interestingly, another group reported that m^{6}A levels are regulated by the miRNA machinery and by miRNAs [82]. In that study, the authors proposed that miRNA regulates m^{6}A formation by modulating METTL3/mRNA binding, presumably in the cytoplasm. However, it is unclear how miRNA-modulated METTL3/mRNA binding affects m^{6}A methylation, since METTL14 is a nuclear protein [76] and m^{6}A methylation likely occurs in the nucleus. Nevertheless, these studies suggest the cellular interaction of two major RNA regulatory mechanisms: m^{6}A mRNA modification and miRNAs. However, detailed mechanisms remain to be investigated.

Concluding Remarks and Future Perspectives

There has been an enormous expansion in our knowledge of m^{6}A modification over the past few years. Nonetheless, fundamental questions relevant to regulation and activity of this modification remain (see Outstanding Questions). For example, we do not yet know why m^{6}A methyltransferases methylate some but not all mRNAs. We also do not yet comprehend what factors control the extent of m^{6}A modification of a particular mRNA. Mechanisms that maintain the balance between formation and removal of m^{6}A are not yet well defined and neither is it understood how m^{6}A-binding proteins compete with the demethylases. While numerous functions of m^{6}A modification are proposed, based largely on genome-wide data, the ultimate test of mutating endogenous m^{6}A sites followed by phenotypic analysis is lacking. In addition, although m^{6}A is present on rRNA, tRNA, small nuclear (sn)RNA, small nucleolar (sno)RNA [83], it is not known whether characterized m^{6}A readers recognize modified RNAs outside the context of polyA RNAs. In short, our journey down the road to understand m^{6}A mechanism and function has only just begun.

Outstanding Questions

Why do m^{6}A methyltransferases methylate some but not all mRNAs? What factors control the extent of m^{6}A modification of a particular mRNA?

What maintains the balance between formation and removal of m^{6}A? How are m^{6}A levels regulated in cells?

Would a characterized m^{6}A mRNA reader recognize m^{6}A-modified tRNA, rRNA, or snoRNA? Is there any cross-talk between different types of RNA through m^{6}A modification?m^{6}A regulates mRNA activities through diverse mechanisms. How do these mechanisms coexist in cells?

Acknowledgments

We thank the NIH for funding P30 CA023168 and R01 GM110090 to J.C.Z.

References

1. Desrosiers, R. *et al.* (1974) Identification of methylated nucleosides in messenger RNA from Novikoff hepatoma cells. *Proc. Natl. Acad. Sci. U.S.A.* 71, 3971–3975
2. Adams, J.M. and Cory, S. (1975) Modified nucleosides and bizarre 5′-termini in mouse myeloma mRNA. *Nature* 255, 28–33
3. Perry, R.P. *et al.* (1975) The methylated constituents of L cell messenger RNA: evidence for an unusual cluster at the 5′ terminus. *Cell* 4, 387–394
4. Wei, C.M. *et al.* (1976) 5′-Terminal and internal methylated nucleotide sequences in HeLa cell mRNA. *Biochemistry* 15, 397–401
5. Keith, G. (1995) Mobilities of modified ribonucleotides on two-dimensional cellulose thin-layer chromatography. *Biochimie* 77, 142–144
6. Zhong, S. *et al.* (2008) MTA is an *Arabidopsis* messenger RNA adenosine methylase and interacts with a homolog of a sex-specific splicing factor. *Plant Cell* 20, 1278–1288

7. Jia, G. *et al.* (2011) N6-methyladenosine in nuclear RNA is a major substrate of the obesity-associated FTO. *Nat. Chem. Biol.* 7, 885–887
8. Furuichi, Y. *et al.* (1975) 5'-Terminal m-7G(5')ppp(5')G-m-p in vivo: identification in reovirus genome RNA. *Proc. Natl. Acad. Sci. U.S. A.* 72, 742–745
9. Wei, C.M. *et al.* (1975) Methylated nucleotides block 5' terminus of HeLa cell messenger RNA. *Cell* 4, 379–386
10. Bokar, J.A. (2005) The biosynthesis and functional roles of methylated nucleosides in eukaryotic mRNA. *Topics Curr. Genet.* 12, 141–177
11. Motorin, Y. *et al.* (2007) Identification of modified residues in RNAs by reverse transcription-based methods. *Methods Enzymol.* 425, 21–53
12. Frommer, M. *et al.* (1992) A genomic sequencing protocol that yields a positive display of 5-methylcytosine residues in individual DNA strands. *Proc. Natl. Acad. Sci. U.S.A.* 89, 1827–1831
13. Meyer, K.D. *et al.* (2012) Comprehensive analysis of mRNA methylation reveals enrichment in 3' UTRs and near stop codons. *Cell* 149, 1635–1646
14. Dominissini, D. *et al.* (2012) Topology of the human and mouse m6A RNA methylomes revealed by m6A-seq. *Nature* 485, 201–206
15. Schwartz, S. *et al.* (2013) High-resolution mapping reveals a conserved, widespread, dynamic mRNA methylation program in yeast meiosis. *Cell* 155, 1409–1421
16. Batista, P.J. *et al.* (2014) m(6)A RNA modification controls cell fate transition in mammalian embryonic stem cells. *Cell Stem Cell* 15, 707–719
17. Schwartz, S. *et al.* (2014) Perturbation of m6A writers reveals two distinct classes of mRNA methylation at internal and 5' sites. *Cell Rep.* 8, 284–296
18. Wang, X. *et al.* (2014) N6-methyladenosine-dependent regulation of messenger RNA stability. *Nature* 505, 117–120
19. Wang, Y. *et al.* (2014) N6-methyladenosine modification destabilizes developmental regulators in embryonic stem cells. *Nat. Cell Biol.* 16, 191–198
20. Chen, K. *et al.* (2015) High-resolution N(6) -methyladenosine (m(6) A) map using photo-crosslinking-assisted m(6) A sequencing. *Angew. Chem.* 54, 1587–1590
21. Ke, S. *et al.* (2015) A majority of m6A residues are in the last exons, allowing the potential for 3' UTR regulation. *Genes Dev.* 29, 2037–2053
22. Linder, B. *et al.* (2015) Single-nucleotide-resolution mapping of m6A and m6Am throughout the transcriptome. *Nat. Methods* 12, 767–772
23. Molinie, B. *et al.* (2016) m(6)A-LAIC-seq reveals the census and complexity of the m(6)A epitranscriptome. *Nat. Methods* 13, 692–698
24. Csepany, T. *et al.* (1990) Sequence specificity of mRNA N6-adenosine methyltransferase. *J. Biol. Chem.* 265, 20117–20122
25. Harper, J.E. *et al.* (1990) Sequence specificity of the human mRNA N6-adenosine methylase in vitro. *Nucleic Acids Res.* 18, 5735–5741
26. Rottman, F.M. *et al.* (1994) N6-adenosine methylation in mRNA: substrate specificity and enzyme complexity. *Biochimie* 76, 1109–1114
27. Zhao, X. *et al.* (2014) FTO-dependent demethylation of N6-methyladenosine regulates mRNA splicing and is required for adipogenesis. *Cell Res.* 24, 1403–1419
28. Ping, X.L. *et al.* (2014) Mammalian WTAP is a regulatory subunit of the RNA N6–methyladenosine methyltransferase. *Cell Res.* 24, 177–189
29. Schibler, U. and Perry, R.P. (1977) The 5'-termini of heterogeneous nuclear RNA: a comparison among molecules of different sizes and ages. *Nucleic Acids Res.* 4, 4133–4149
30. Meyer, K.D. *et al.* (2015) 5' UTR m(6)A promotes cap-independent translation. *Cell* 163, 999–1010
31. Li, Y. *et al.* (2015) Genome-wide detection of high abundance N6-methyladenosine sites by microarray. *RNA* 21, 1511–1518
32. Engel, J.D. and von Hippel, P.H. (1974) Effects of methylation on the stability of nucleic acid conformations: studies at the monomer level. *Biochemistry* 13, 4143–4158
33. Engel, J.D. and von Hippel, P.H. (1978) Effects of methylation on the stability of nucleic acid conformations. Studies at the polymer level. *J. Biol. Chem.* 253, 927–934
34. Micura, R. *et al.* (2001) Methylation of the nucleobases in RNA oligonucleotides mediates duplex-hairpin conversion. *Nucleic Acids Res.* 29, 3997–4005
35. Kierzek, E. (2003) The thermodynamic stability of RNA duplexes and hairpins containing N6-alkyladenosines and 2-methylthio-N6-alkyladenosines. *Nucleic Acids Res.* 31, 4472–4480
36. Roost, C. *et al.* (2015) Structure and thermodynamics of N6-methyladenosine in RNA: a spring-loaded base modification. *J. Am. Chem. Soc.* 137, 2107–2715
37. Harcourt, E.M. *et al.* (2013) Identification of a selective polymerase enables detection of N(6)-methyladenosine in RNA. *J Am Chem Soc* 135, 19079–19082
38. Vilfan, I.D. *et al.* (2013) Analysis of RNA base modification and structural rearrangement by single-molecule real–time detection of reverse transcription. *J. Nanobiotechnol.* 11, 8
39. Dai, Q. *et al.* (2007) Identification of recognition residues for ligation-based detection and quantitation of pseudouridine and N6-methyladenosine. *Nucleic Acids Res.* 35, 6322–6329
40. Liu, N. *et al.* (2013) Probing N6-methyladenosine RNA modification status at single nucleotide resolution in mRNA and long noncoding RNA. *RNA* 19, 1848–1856
41. Tuck, M.T. (1992) Partial purification of a 6-methyladenine mRNA methyltransferase which modifies internal adenine residues. *Biochem. J.* 288, 233–240
42. Bokar, J.A. *et al.* (1994) Characterization and partial purification of mRNA N6-adenosine methyltransferase from HeLa cell nuclei. Internal mRNA methylation requires a multisubunit complex. *J. Biol. Chem.* 269, 17697–17704
43. Bokar, J.A. *et al.* (1997) Purification and cDNA cloning of the AdoMet-binding subunit of the human mRNA (N6-adenosine)-methyltransferase. *RNA* 3, 1233–1247
44. Liu, J. *et al.* (2014) A METTL3-METTL14 complex mediates mammalian nuclear RNA N6-adenosine methylation. *Nat. Chem. Biol.* 10, 93–95
45. Bujnicki, J.M. *et al.* (2002) Structure prediction and phylogenetic analysis of a functionally diverse family of proteins homologous to the MT-A70 subunit of the human mRNA:m(6)A methyltransferase. *J. Mol. Evol.* 55, 431–444
46. Sledz, P. and Jinek, M. (2016) Structural insights into the molecular mechanism of the m(6)A writer complex. *eLife* 5, e18434
47. Wang, P. *et al.* (2016) Structural basis for cooperative function of Mettl3 and Mettl14 methyltransferases. *Mol. Cell* 63, 306–317
48. Wang, X. *et al.* (2016) Structural basis of N-adenosine methylation by the METTL3–METTL14 complex. *Nature* 534, 575–578
49. Agarwala, S.D. *et al.* (2012) RNA methylation by the MIS complex regulates a cell fate decision in yeast. *PLoS Genet.* 8, e1002732
50. Zheng, G. *et al.* (2013) ALKBH5 is a mammalian RNA demethylase that impacts RNA metabolism and mouse fertility. *Mol. Cell* 49, 18–29
51. Gerken, T. *et al.* (2007) The obesity-associated FTO gene encodes a 2-oxoglutarate-dependent nucleic acid demethylase. *Science* 318, 1469–1472
52. Jia, G. *et al.* (2008) Oxidative demethylation of 3-methylthymine and 3-methyluracil in single-stranded DNA and RNA by mouse and human FTO. *FEBS Lett.* 582, 3313–3319
53. Feng, C. *et al.* (2014) Crystal structures of the human RNA demethylase Alkbh5 reveal basis for substrate recognition. *J. Biol. Chem.* 289, 11571–11583
54. Chen, W. *et al.* (2014) Crystal structure of the RNA demethylase ALKBH5 from zebrafish. *FEBS Lett.* 588, 892–898
55. Han, Z. *et al.* (2010) Crystal structure of the FTO protein reveals basis for its substrate specificity. *Nature* 464, 1205–1209
56. Chen, B. *et al.* (2012) Development of cell-active N6-methyladenosine RNA demethylase FTO inhibitor. *J. Am. Chem. Soc.* 134, 17963–17971
57. Xu, C. *et al.* (2014) Structural basis for selective binding of m6A RNA by the YTHDC1 YTH domain. *Nat. Chem. Biol.* 10, 927–929
58. Wang, X. *et al.* (2015) N(6)-methyladenosine Modulates Messenger RNA Translation Efficiency. *Cell* 161, 1388–1399

59. Xiao, W. *et al.* (2016) Nuclear m(6)A reader YTHDC1 regulates mRNA splicing. *Mol. Cell* 61, 507–519
60. Zhang, Z. *et al.* (2010) The YTH domain is a novel RNA binding domain. *J. Biol. Chem.* 285, 14701–14710
61. Theler, D. *et al.* (2014) Solution structure of the YTH domain in complex with N6-methyladenosine RNA: a reader of methylated RNA. *Nucleic Acids Res.* 42, 13911–13919
62. Zhu, T. *et al.* (2014) Crystal structure of the YTH domain of YTHDF2 reveals mechanism for recognition of N6-methyladenosine. *Cell Res* 24, 1493–1496
63. Hashimoto, H. *et al.* (2012) Recognition and potential mechanisms for replication and erasure of cytosine hydroxymethylation. *Nucleic Acids Res.* 40, 4841–4849
64. Alarcon, C.R. *et al.* (2015) HNRNPA2B1 is a mediator of m(6)A-dependent nuclear RNA processing Events. *Cell* 162, 1299–1308
65. Bachellerie, J.P. *et al.* (1978) Biosynthesis and utilization of extensively undermethylated poly(A)+ RNA in CHO cells during a cycloleucine treatment. *Nucleic Acids Res.* 5, 2927–2943
66. Geula, S. *et al.* (2015) Stem cells. m6A mRNA methylation facilitates resolution of naive pluripotency toward differentiation. *Science* 347, 1002–1006
67. Du, H. *et al.* (2016) YTHDF2 destabilizes m(6)A-containing RNA through direct recruitment of the CCR4–NOT deadenylase complex. *Nat. Commun.* 7, 12626
68. Kennedy, E.M. *et al.* (2016) Posttranscriptional m(6)A editing of HIV-1 mRNAs enhances viral gene expression. *Cell Host Microbe* 19, 675–685
69. Tirumuru, N. *et al.* (2016) N6-methyladenosine of HIV-1 RNA regulates viral infection and HIV-1 Gag protein expression. *eLife* 5, e15528
70. Rouskin, S. *et al.* (2014) Genome-wide probing of RNA structure reveals active unfolding of mRNA structures in vivo. *Nature* 505, 701–705
71. Ding, Y. *et al.* (2014) In vivo genome-wide profiling of RNA secondary structure reveals novel regulatory features. *Nature* 505, 696–700
72. Spitale, R.C. *et al.* (2015) Structural imprints in vivo decode RNA regulatory mechanisms. *Nature* 519, 486–490
73. Liu, N. *et al.* (2015) N(6)-methyladenosine-dependent RNA structural switches regulate RNA-protein interactions. *Nature* 518, 560–564
74. Zhou, J. *et al.* (2015) Dynamic m(6)A mRNA methylation directs translational control of heat shock response. *Nature* 526, 591–594
75. Zou, S. *et al.* (2016) N(6)-Methyladenosine: a conformational marker that regulates the substrate specificity of human demethylases FTO and ALKBH5. *Sci. Rep.* 6, 25677
76. Lin, S. *et al.* (2016) The m(6)A methyltransferase METTL3 promotes translation in human cancer cells. *Mol. Cell* 62, 335–345
77. Choi, J. *et al.* (2016) N(6)-methyladenosine in mRNA disrupts tRNA selection and translation-elongation dynamics. *Nat. Struct. Mol. Biol.* 23, 110–115
78. Ben-Haim, M.S. *et al.* (2015) FTO: linking m6A demethylation to adipogenesis. *Cell Res.* 25, 3–4
79. Huang, Y. *et al.* (2004) A molecular link between SR protein dephosphorylation and mRNA export. *Proc. Natl. Acad. Sci. U. S.A.* 101, 9666–9670
80. Lai, M.C. and Tarn, W.Y. (2004) Hypophosphorylated ASF/SF2 binds TAP and is present in messenger ribonucleoproteins. *J. Biol. Chem.* 279, 31745–31749
81. Alarcon, C.R. *et al.* (2015) N6-methyladenosine marks primary microRNAs for processing. *Nature* 519, 482–485
82. Chen, T. *et al.* (2015) m(6)A RNA methylation is regulated by microRNAs and promotes reprogramming to pluripotency. *Cell Stem Cell* 16, 289–301
83. Cantara, W.A. *et al.* (2011) The RNA Modification Database, RNAMDB: 2011 update. *Nucleic Acids Res.* 39, D195–D201